Article

Galactosylation of Cosmetic Preservatives to Reduce Skin Permeation and Cytotoxicity

Muhammad Raza , Su-Hong Kim , Min-Sik Kang , Jae-Hyeob Kim , Gi-Seong Moon , Arunporn Itharat , Jun-Sub Kim , Hyang-Yeol Lee *

Posted Date: 4 May 2026

doi: 10.20944/preprints202605.0095.v1

Keywords: cosmetics; preservatives; enzymatic galactosylation; β-galactosidase; skin permeability; cytotoxicity; Franz diffusion cell

 doi:10.20944/preprints202605.0095.v1

Article

Galactosylation of Cosmetic Preservatives to Reduce Skin Permeation and Cytotoxicity

Muhammad Raza [1], Su-Hong Kim [1], Min-Sik Kang [1], Jae-Hyeob Kim [1], Gi-Seong Moon [1], Arunporn Itharat [2], Jun-Sub Kim [1] and Hyang-Yeol Lee [1,*]

[1] Department of Biotechnology, Korea National University of Transportation, 61 Daehak-ro, Jeungpyeong-gun, Chungbuk 368-701, Republic of Korea

[2] Department of Applied Thai Traditional Medicine and Center of Excellence in Applied Thai Traditional Medicine Research (CEATMR), Faculty of Medicine, Thammasat University, Klongluang, Patumthani, 12120, Thailand

* Correspondence: hyl@ut.ac.kr; Tel.: 82-43-820-5252, Fax: 82-43-820-5252

Abstract

Cosmetic preservatives should have reduced percutaneous absorption to lower the risk of systemic exposure and skin irritation. In this work, *Escherichia coli* β-galactosidase was used to enzymatically modify several of the commonly used cosmetic preservatives to produce their corresponding galactosylated derivatives: benzyl alcohol β-D-galactopyranoside **7**, 2-phenoxyethanol β-D-galactopyranoside **8**, chlorphenesin β-D-galactopyranoside **9**, 1,2-hexanediol β-D-galactopyranoside **10**, 1,2-octanediol β-D-galactopyranoside **11**, and 2-phenylethyl β-D-galactopyranoside **12**. HPLC and NMR spectroscopy were used to analyze the synthesized derivatives. The Franz diffusion cell assay was used to evaluate skin penetration. 2-phenoxyethanol (PE), chlorphenesin (CPN), and 2-phenylethanol (PhE), exhibited measurable skin penetration with flux values ranging from 3.82 to 7.34 $\mu g \cdot h^{-1} \cdot cm^{-2}$ and permeability coefficients (Kp) between 1.38 and 3.00 $\times 10^{-3}$ $cm \cdot h^{-1}$. In contrast, their galactosylated derivatives showed markedly reduced permeation under the same experimental conditions. Moreover, brine shrimp lethality assays indicated that galactosylated derivatives had significantly higher LD_{50} values (1.6–2.1 mg/mL) than their parent compounds (0.1–0.79 mg/mL), suggesting lower cytotoxicity. These findings suggest that enzymatic galactosylation can significantly decrease skin permeability and the toxicity of cosmetic preservatives, highlighting its potential as a strategy to improve the safety of cosmetic ingredients.

Keywords: cosmetics; preservatives; enzymatic galactosylation; β-galactosidase**;** skin permeability; cytotoxicity; Franz diffusion cell

1. Introduction

Cosmetic preservatives are commonly used in personal care products to prevent microbiological contamination and ensure product stability during storage and use. However, the safety of preservatives has become a major concern because several commonly used chemicals can penetrate the skin and cause irritation, allergic reactions, or systemic exposure with continuous usage[1–3].

Many preservatives, such as 2-phenoxyethanol, chlorphenesin, benzyl alcohol, and 2-phenylethanol, are frequently used in cosmetic formulations due to their broad antibacterial properties and formulation compatibility[4–6]. Some of these compounds have been shown in previous studies to exhibit varying degrees of skin barrier penetration despite their effectiveness[7,8].

A particular approach to reducing the epidermal penetration of small molecules is chemical or enzymatic process that increases their hydrophilicity and molecular size[9–11]. Glycosylation, particularly galactosylation, has been widely used in pharmacological and biochemical research to modify the physicochemical properties of bioactive compounds[12] making less permeable through the lipophilic layers of the epidermal barrier[13]. Enzymatic galactosylation has several advantages

 doi:10.20944/preprints202605.0095.v1

over traditional chemical synthesis, including excellent specificity, mild reaction conditions, and environmentally friendly process. β-galactosidase from *Escherichia coli* is commonly used as a biocatalyst in transgalactosylation strategies to produce galactosylated derivatives[14,15].

In this study, galactosylated derivatives of several widely used cosmetic preservatives were produced via enzymatic modification. Chromatographic and spectroscopic techniques were used to characterize the modified compounds. Additionally, Franz diffusion cell studies were used to assess the skin penetration of the parent compounds and their galactosylated derivatives. Brine shrimp lethality experiment was also used to measure cytotoxicity (LD_{50}). The purpose of this study was to determine whether galactosylation may improve the safety profile of cosmetic preservatives for cosmetic applications by lowering their skin permeability and toxicity. The enzymatic galactosylation of conventional preservatives benzyl alcohol (BnOH) **1**, 2-phenoxyethanol (PE) **2**, chlorphenesin (CPN) **3**, 1,2-hexanediol (HD) **4**, and 1,2-octanediol (OD) **5** and 2-phenylethanol (PhE) **6** using *E. coli*, β-galactosidase resulted in the yielding of their corresponding galactosylated derivatives **7-12**, as shown in Figure 1.

 doi:10.20944/preprints202605.0095.v1

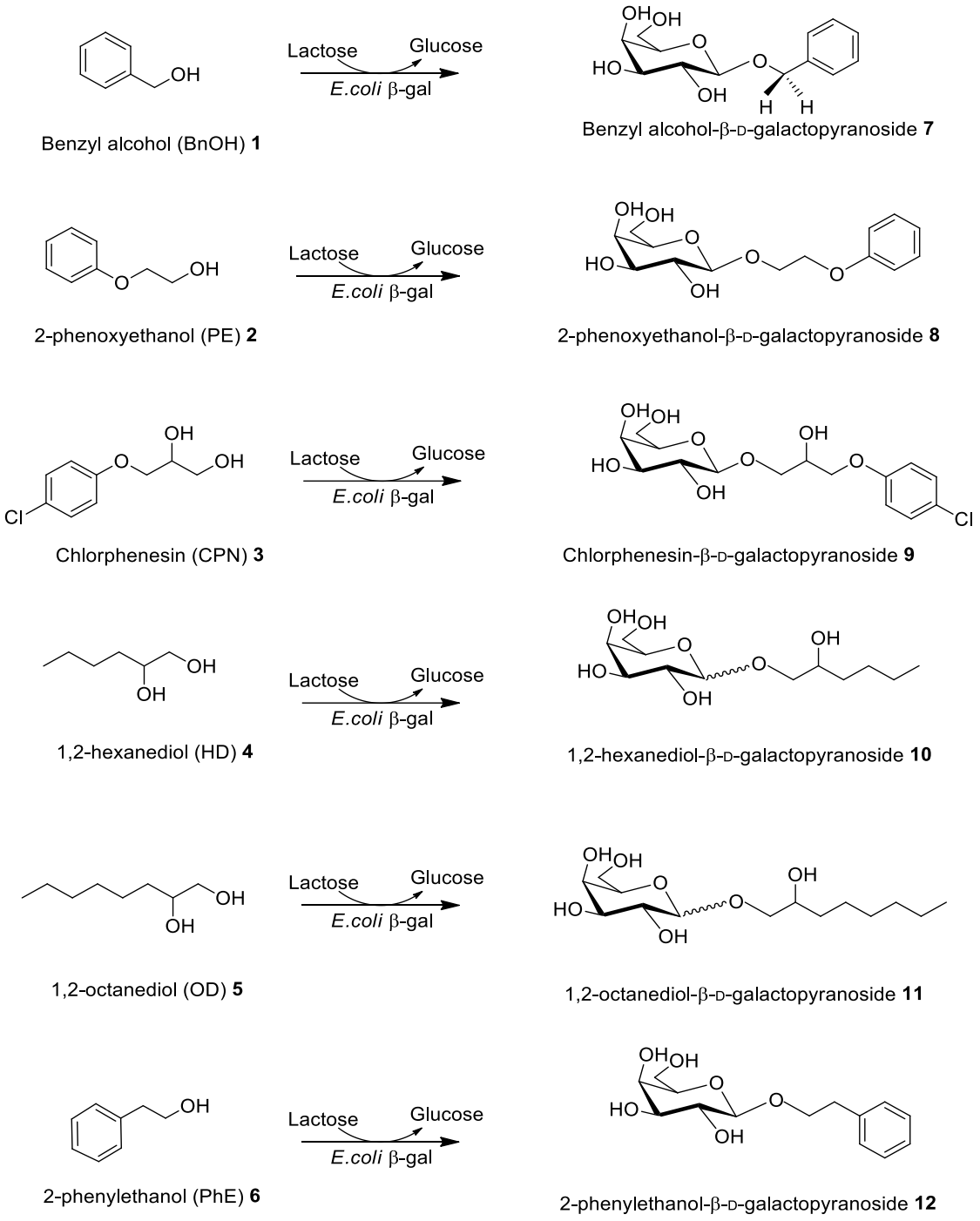

Figure 1. Galactosylation-mediated transformation of benzyl alcohol **1**, 2-phenoxyethanol **2**, chlorphenesin **3**, 1,2-hexanediol **4**, 1,2-octanediol **5**, and 2-phenylethanol **6** into β-D-galactosylated compounds **7**-**12**.

Previously we synthesized and characterized 1,2-octanediol β-D-galactopyranoside **11** and benzyl alcohol β-D-galactopyranoside **7**[16], 2-phenoxyethanol β-D-galactopyranoside **8**[17], chlorphenesin β-D-galactopyranoside **9**[18], and 1,2-hexanediol β-D-galactopyranoside **10**[19] using *Escherichia coli* expressing β-galactosidase. These galactoside derivatives showed improved water solubility, reduced cytotoxicity, and sustained antimicrobial activity, highlighting their potential as safer and more effective cosmetic preservatives[17].

Dermal permeability of chemical substances can be evaluated using Franz diffusion cell assay[20]. Conventional cosmetic preservatives CPN, PE, and PhE are commonly used in cosmetics due to their strong antimicrobial activity, but their ability to penetrate the skin may lead to cytotoxic and systemic effects[21].

 doi:10.20944/preprints202605.0095.v1

Cytotoxicity of non-galactosylated and galactosylated compounds was evaluated using the brine shrimp lethality assay. The 24-hour toxicity was determined by calculating LD_{50} values, representing the concentration required to kill 50% of the shrimp larvae, following a standard protocol. Experiments were performed in five independent sets, each conducted in triplicate, to ensure reproducibility and reliability of results[22].

The successful synthesis of β-D-galactopyranoside derivatives of benzyl alcohol, 2-phenoxy ethanol, chlorphenesin, 1,2-hexanediol, 1,2-octanediol, and 2-phenylethanol was confirmed by LC–MS and $^{1}H/^{13}C$ NMR analysis. The spectra showed the expected characteristic signals corresponding to both the sugar and aglycone moieties, confirming the structures of the synthesized derivatives[23,24].

2. Material and Method

The following compounds were purchased from commercial suppliers: 2-phenoxyethanol (PE) (Fluka), 2-phenylethanol (PhE) (Sigma-Aldrich, USA), chlorphenesin (CPN) (CosMol Co., Siheung, Korea), 1,2-hexanediol (Samchun), 1,2-octanediol (ThermoScientific, UK), and methyl paraben (Sigma-Aldrich, India). Phosphate-buffered saline (PBS) solution was prepared by dissolving one PBS tablet (Sigma-Aldrich, USA) in 200 mL of triple-distilled water. Thin-layer chromatography (TLC) plates (DC Kiesel gel 60 F254) were obtained from Merck Millipore, USA, and silica gel 60 (0.040–0.063mm) was also acquired from Merck Millipore for chromatographic applications.

For skin permeability experiments, the Strat-M™ Membrane (Transdermal Diffusion Test Model) was used. HPLC analysis was performed using a Waters e2695 model. The solvents used included anhydrous ethanol and methanol (Daesung, Siheung, Korea) and acetonitrile (99.9%) (Samjeon, Seoul, Korea). The Franz Diffusion cell assay equipment was obtained from BNC Tech, Daejeon, Korea, and used for skin permeability experiments.

2.1. Preparation of Culture Medium

The culture medium was made by dissolving yeast extract (20 g), glycerol (20 g), KH_2PO_4 (2.3 g), and $Na_2HPO_4.12H_2O$ (25.75 g) in distilled water. The final volume was adjusted to 1 L with distilled water under magnetic stirring.

2.2. Sterilization Procedure

100 mL of the medium for seed culture preparation was put into a 500 mL Erlenmeyer flask, and the remaining 900 mL was put into the fermenter for main culture. The Erlenmeyer flask was sealed with a silicon stopper and wrapped in aluminum foil. The fermenter was assembled as per the manufacturer's instructions.

Arabinose (1%, 10 mL) and fucose (0.5%, 10 mL) solutions were prepared in 15 mL conical tubes, loosely sealed, and covered with foil before sterilization. Aluminum foil was also placed over 1000 µL and 200 µL micropipette tip boxes before autoclaving. All equipment used to handle microorganisms was sterilized before the experiment.

2.3. Synthesis of Galactosylated Compounds Using β-Galactosidase

β-galactosidase was heterologously expressed in recombinant *E. coli* under the control of the araBAD promoter using the pBAD/Myc-His/lacZ vector (7.2 kb; Invitrogen, Carlsbad, CA, USA). After fermentation, the enzyme was purified from the bacterial cells for subsequent reactions.

For the synthesis of 2-phenoxyethanol-galactoside (PE-gal), PE (940 µL, 75 mM) was mixed with 50 mM phosphate-buffered saline (PBS, pH 7.0), and the total volume was adjusted to 100 mL. Lactose (30 g) was dissolved using a sonicator, followed by the addition of β-galactosidase (1200 U). The reaction was incubated at 37°C with shaking at 200 rpm for 48 h. Other galactosylated derivatives were synthesized using the same method with different substrates, including 1,2-hexanediol (878 µL), 1,2-octanediol (1,218 µL), 2-phenylethanol (898 µL), and chlorphenesin (1.84 g).

 doi:10.20944/preprints202605.0095.v1

2.4. Fractionation and Sugar Precipitation

A separatory funnel and ethyl acetate (1:1, v/v) were used to extract nonpolar components from the reaction mixture. In the aqueous phase, sugars and glycosylated products were collected. Residual sugars derived from lactose were precipitated using ethanol or acetonitrile (2:1 v/v). The supernatant was concentrated using a rotary evaporator. This process was repeated until sugars could no longer be detected by thin-layer chromatography (TLC).

2.5. Purification by Column Chromatography

The partially purified reaction mixture was subsequently separated using silica gel column chromatography. Acetonitrile/water (97:3, v/v) was the eluent. TLC analysis of the resulting fractions was used to identify the galactosylated products. TLC analyses and Rf values of the standard compounds and synthesized galactoside are included in Figure 2**.**

2.6. Chromatographic Requirements for HPLC Analysis

High-performance liquid chromatography (HPLC) was performed to analyze PE **2**, PE-gal **8**, CPN **3**, CPN-gal **9**, PhE **6**, and PhE-gal **12**. A C18 column (Phenomenex Gemini, 5 µm, 110 Å, 150 × 4.6 mm) was used with a 43-min gradient program the injection volume was 100 µL. Solvent A was distilled water, and solvent B was acetonitrile (ACN). The flow rate was kept at 1.0 mL/min. Detection wavelengths were set at 280 nm for PE, PE-gal, PhE, and PhE-gal, and at 210 nm for CPN and CPN-gal, as shown in Table 1.

All compounds were successfully detected using a photodiode-array (PDA) detector.

Table 1. HPLC method and condition.

Compound(s)	Column	Mobile Phase	Flow Rate	Wavelength (nm)	Temp (°C)	Method
2, 8, 6, 12	Phenomenex Gemini 5 µm C18 110Å 150×4.6 mm	A: Distilled Water, B: ACN	1.0 mL/min	280	30°C	Gradient
3, 9	Phenomenex Gemini 5 µm C18 110Å 150×4.6 mm	A: Distilled Water, B: ACN	1.0 mL/min	210	30°C	Gradient

2.7. Evaluation of Skin Permeation Using Franz Diffusion Cell Assay

The skin penetration variations in 2-phenoxyethanol (PE), 2-phenylethanol (PhE), chlorphenesin (CPN), and their corresponding galactosylated derivatives (PE-gal **8**, PhE-gal **12**, and CPN-gal **9**) were evaluated using a Franz diffusion cell system. Strat-M™ synthetic membranes (25 mm diameter, thickness 300 µm; Millipore, USA) were used as the artificial skin model for the Franz diffusion cell experiments. The effective diffusion area of the membrane was 0.64 cm^2.The receptor medium consisted of ethanol: PBS (1:1, v/v, 75 mM) to ensure sufficient solubility. To prevent air entrapment, the receptor chamber was filled with the receptor medium after the Strat-M™ membrane was carefully positioned between the donor and receptor compartments.

Each donor chamber received 2 mL of the test solution (75 mM). Diffusion cells were maintained at 32 °C to mimic the normal skin temperature. To maintain uniform concentration and encourage consistent diffusion, the receptor phase was continually stirred using a magnetic stir bar. The start of stirring was considered time zero. Aliquots (100 µL) were removed from the sampling port at 12, 24, 36, and 48 hours, and an equal volume of fresh receptor media was quickly reintroduced to maintain the volume. The collected samples were stored at 4°C for 12 hours before being evaluated using high-performance liquid chromatography (HPLC).

 doi:10.20944/preprints202605.0095.v1

This experimental methodology allowed a direct and quantitative comparison of the skin penetration effects of conventional preservatives and their corresponding galactosylated derivatives. Calibration curves for PE/PE-gal, PhE/PhE-gal, and CPN/CPN-gal are included in the supplementary Information Figure S1**.**

2.8. Calculation of Flux and Permeability Coefficient (Kp)

The permeability coefficient (Kp) was calculated by dividing the steady-state flux by the initial concentration of the test compound. Flux values ($\mu g \cdot cm^{-2} \cdot h^{-1}$) were obtained from the linear portion of the cumulative permeation over time profile[25–27].

Parent compounds (PE, CPN, and PhE), clear steady-state regions were observed, allowing reliable calculation of both flux and Kp values. In comparison, small chromatographic signals corresponding to the galactosylated derivatives (PE-gal, CPN-gal, and PhE-gal) were detected in the receptor phase, despite their concentrations remaining below zero (0). Therefore, reliable steady-state flux and permeability coefficient (Kp) values could not be determined for these compounds under the experimental conditions.

The calculated flux and Kp values for the parent compounds, along with limit of quantification (LOQ) based reporting for the galactosylated derivatives, are presented in the Results section.

3. Cytotoxicity Assessment Using Brine Shrimp Lethality Assay

The *Artemia salina* are then used to calculate the toxicity $LD_{50,}$ a minimal amount of tested substance, inexpensive, safe or does not require feeding during the experiment[28]. Various hazardous materials, including metal complexes, bioactive compounds, natural extracts, and pesticide nanoparticles, have been tested using *Artemia salina* species[29]. The nauplii stage is highly sensitive to pollutants, making it an appropriate model for acute toxicity testing[30,31]. In this study, lethality was found to be directly proportional to the concentration of the tested compounds[32].

The cysts of *Artemia salina* used in the toxicity assay were obtained from Ocean Nutrition, Artificial seawater required for hatching was prepared using reef plus marine salt (Aqua Ocean). Aeration of the culture system was provided by an Amazone power air pump (Az-A1, 2.5 W). A soft light source, such as a 7W fluorescent lamp, was used to support optimal hatching conditions. The incubation system was maintained at 28–30°C to ensure proper growth and survival of the brine shrimp. Origin software (OriginLab, 2024) was used for data recording, graphical analysis, and calculation of experimental results.

3.1. Hatching of Artemia salina

Artificial seawater was prepared by dissolving sea salt (35 $g \cdot L^{-1}$) in 1000 mL of distilled water, followed by the addition of *Artemia salina* cysts (2 $g \cdot L^{-1}$). The mixture was aerated using an air pump and maintained at room temperature under continuous illumination for 48 h. Within 24–48 h, the cysts hatched and nauplii developed from the eggshells. The hatched nauplii were collected from the illuminated side of the beaker, as they naturally migrate toward light.

3.2. Toxicity Assay Procedure

LD_{50} values of the test compounds were determined using 24-well plate. A concentration range of 0.1-2 mg/mL or 0.1-3 mg/mL was prepared, with three replicates per concentration. Each well contained a final volume of 1 mL consisting of the test solution and 12-15 nauplii. The plates were incubated at 28-30°C for 24 h. After incubation, nauplii mortality was assessed under a stereoscope. Larvae were considered alive if they displayed internal or external movement within a 10-sec observation period.

The number of dead larvae was counted, and the percentage of mortality was calculated using the formula:

$$\text{Mortality} = \text{Number of dead nauplii} / \text{Total number of nauplii} \times 100\%$$

 doi:10.20944/preprints202605.0095.v1

This method allowed for a precise evaluation of the toxic effects of the tested compounds on *Artemia salina* larvae.

4. Results and Discussion

4.1. Silica Gel Column Chromatography

TLC confirmed the synthesis of galactosylated compounds after 48 h. The purified mixture was separated by silica gel column chromatography using acetonitrile and water (97:3, v/v) as the eluent. A volume of 1.5 µL of each sample was loaded onto the TLC plate, and the plate was dried to visualize the bands. The yield of the isolated product was 14.3%. TLC analysis further confirmed the formation of the product. Analysis performed after 30–48 h indicated maximum product formation.

4.2. TLC Analysis of Reaction Products

Reaction products were analyzed using thin-layer chromatography (TLC). Samples were spotted on silica gel plates (20 × 10 cm) and developed with acetonitrile and water (97:3, v/v). Visualization was performed using $KMnO_4$ staining solution containing $KMnO_4$ (1.5 g), K_2CO_3 (10 g), and 10% NaOH (1.25 mL) in 200 mL distilled water. The Rf values obtained were as follows:
CPN (0.815), CPN-gal (0.482), PhE (0.800), PhE-gal (0.662), PE (0.846), PE-gal (0.692), HD (0.783), HD-gal (0.578), OD (0.771), OD-gal (0.602). These matched the band arrangement shown in Figure 2.

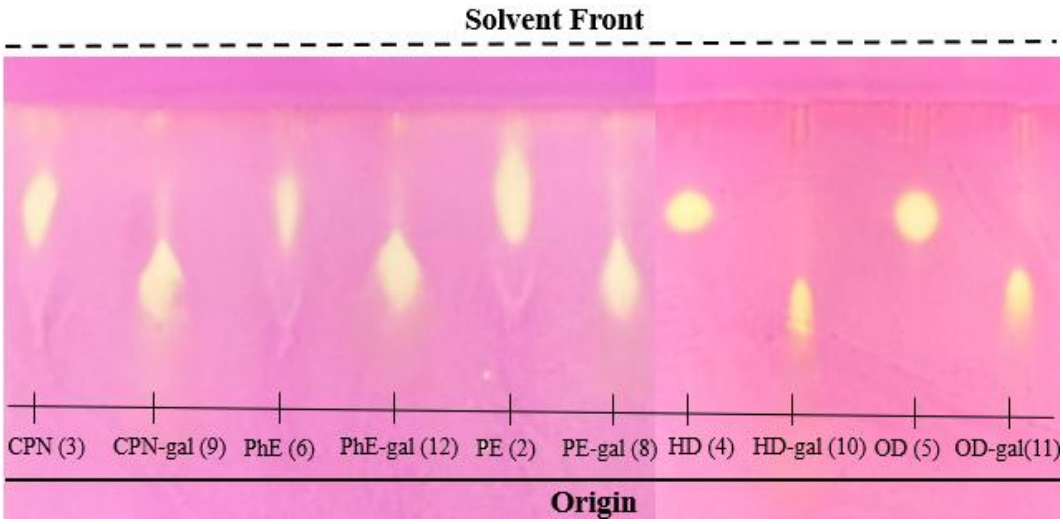

Figure 2. TLC analysis of starting compounds and their corresponding galactosylated derivatives. Samples are arranged based on increasing polarity from left to right.

4.3. Skin Permeation Analysis by Franz Diffusion Cell

a) PE and PE-gal

The skin permeability of non-galactosylated 2-phenoxyethanol (PE) and its galactosylated derivative (PE-gal) was evaluated using Franz diffusion cells at 32°C with Strat-M™ synthetic membranes.

The standard PE showed a retention time (RT) of approximately 12–13 min throughout the analysis. In contrast, PE-gal eluted earlier at around 6–7 min under the applied gradient conditions, reflecting its increased polarity due to galactosylation. The consistent retention times for both compounds confirm their chemical stability during analysis.

The permeation profiles of PE (A1) and PE-gal (B1) further exhibited differences in membrane transport behavior. PE (A1) showed a gradual increase in permeation across the Strat-M™ membrane over time, indicating efficient diffusion. In contrast, PE-gal (B1) produced only weak chromatographic signals in the receptor phase. Although these signals increased slightly over time,

 doi:10.20944/preprints202605.0095.v1

the concentration remained below LOQ under the experimental conditions, preventing reliable calculation of flux and permeability coefficient values as shown in Figure 3.

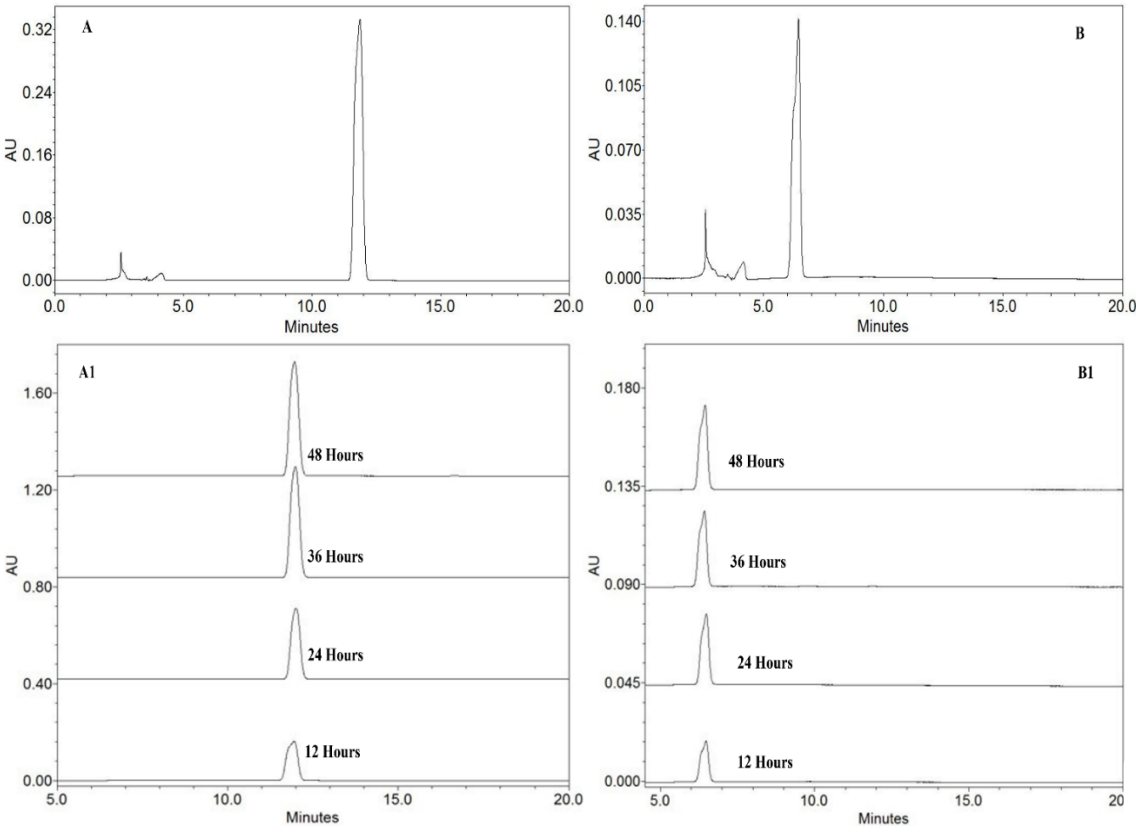

Figure 3. HPLC chromatograms of PE (A) and PE-gal (B) and their time-dependent permeation profiles across Strat-M™ membranes obtained using the Franz diffusion cell system (A1–B1).

b) CPN, CPN-gal

High-performance liquid chromatography (HPLC) was used to evaluate the stability and retention times of CPN and its galactosylated derivative (CPN-gal). In addition, the skin permeation behavior of the CPN (A1) and the CPN-gal (B1) at 32°C was examined using Franz diffusion cells equipped with Strat-M™ membranes, and the collected receptor-phase aliquots were analyzed by HPLC.

The chromatograms showed that the retention time (RT) of chlorphenesin (CPN) remained stable at approximately 8–9 min throughout the experiment, confirming its chemical stability. In contrast, CPN-gal eluted earlier at about 4–5 min due to its higher polarity.

CPN-gal exhibited constant retention time during the permeation experiment, while the peak intensity gradually increased from 12 to 48 h. Throughout the experiment, there were few chromatographic signals that matched CPN-gal, but the levels remained minimum. It was therefore unable to calculate the values of the permeability coefficient and steady state flux as shown in Figure 4.

 doi:10.20944/preprints202605.0095.v1

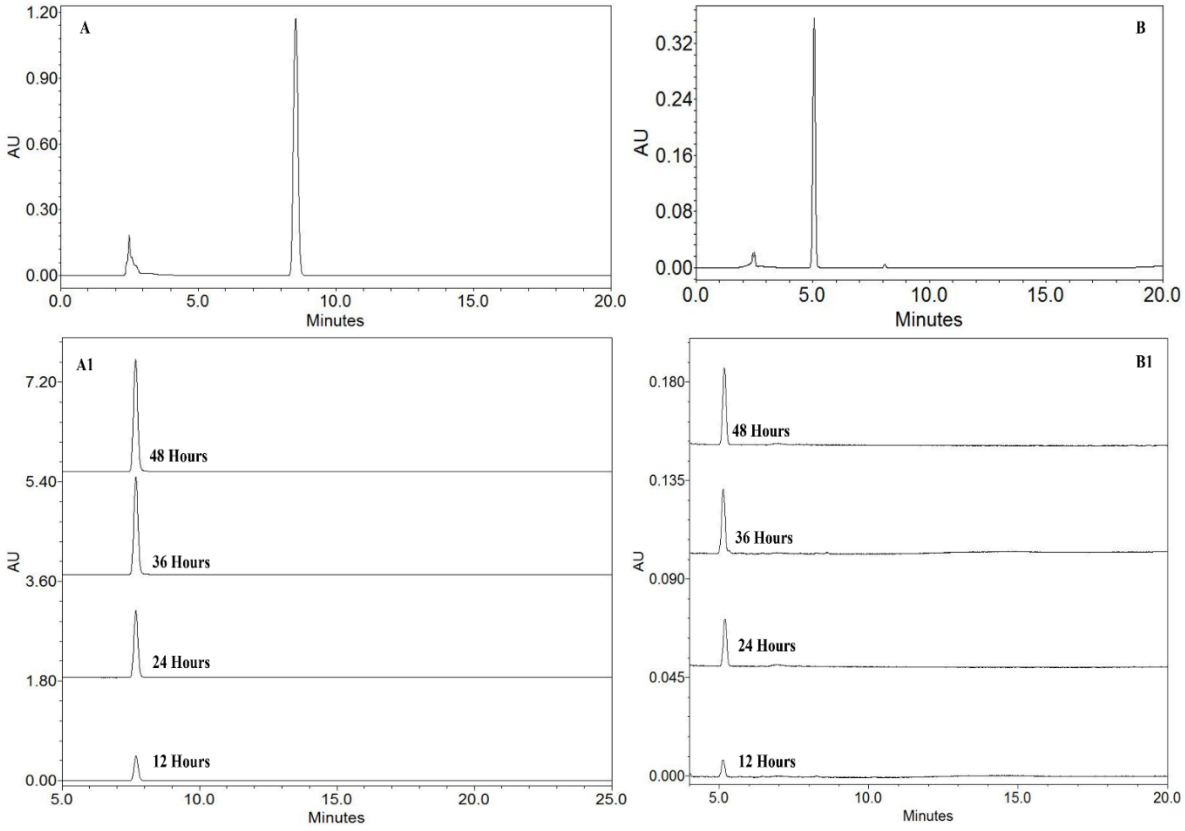

Figure 4. HPLC chromatograms of CPN (A) and CPN-gal (B) and their time-dependent permeation profiles across Strat-M™ membranes obtained using the Franz diffusion cell system (A1–B1).

c) PhE, PhE-gal

High-performance liquid chromatography (HPLC) analysis showed that PhE (A) exhibited a consistent retention time (RT) of approximately 11 min throughout the experiment, confirming its chemical stability. In contrast, PhE-gal (B) eluted earlier at around 5 min due to its higher polarity. During the permeation study, the chromatograms of PhE-gal (B1) in the receptor phase displayed a constant retention time, while the peak intensity gradually increased from 36 to 48 h, indicating a time-dependent increase in concentration. No shift in retention time or additional peaks was observed, suggesting the absence of chemical transformation. However, the concentration remained below the limit under the experimental conditions, making it difficult to calculate precise flux and permeability coefficient values as shown in Figure 5.

 doi:10.20944/preprints202605.0095.v1

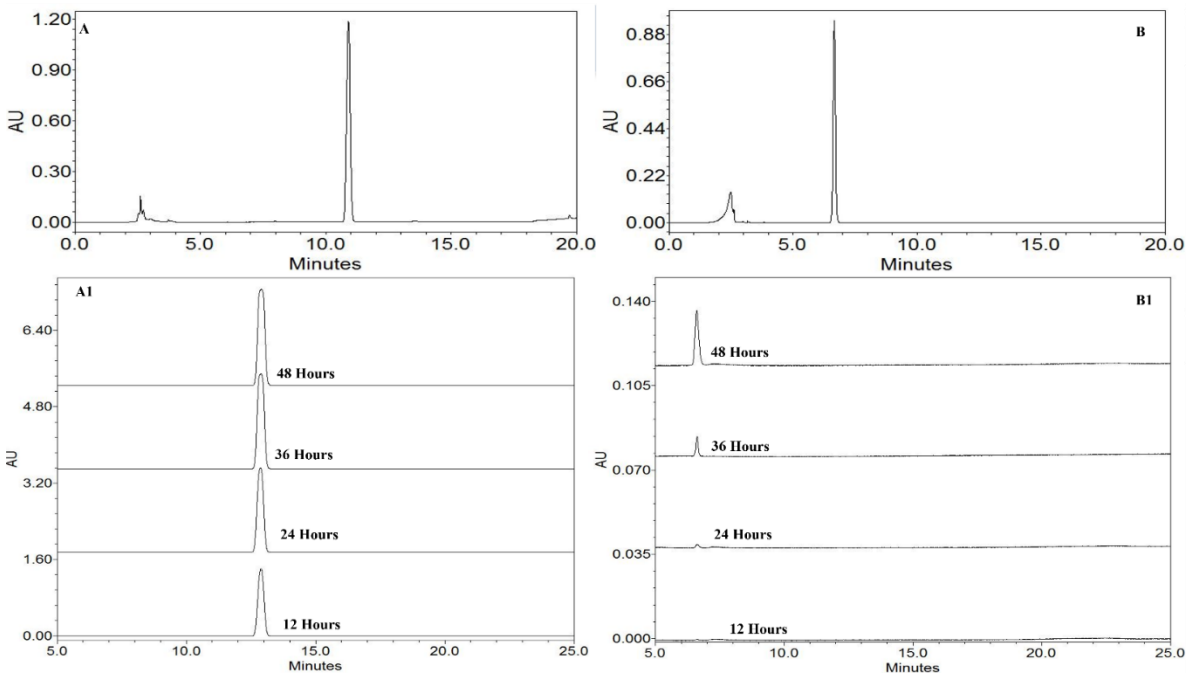

Figure 5. HPLC chromatograms of PhE (A) and PhE-gal (B) and their time-dependent permeation profiles across Strat-M™ membranes obtained using the Franz diffusion cell system (A1–B1).

The representative chromatograms were adjusted to start at 0 min as shown in Figures 3–5. Minor peaks observed in the early region (0–5 min) correspond to the solvent front or void volume signals. Since negligible permeation occurs in this region, slight adjustment of the time scale was applied in some chromatograms to improve clarity of presentation.

4.3. Effect of Galactosylation on Transdermal Flux and Kp

In the Franz diffusion cell assay, galactosylation significantly reduced the transdermal permeation of the compounds. The non-galactosylated compounds that shown observable steady-state flux values over the Strat-M™ membrane were 2-phenoxyethanol, chlorphenesin, and 2-phenylethanol. The initially linear portion of the permeation profile (0–8 h) reflects the steady-state diffusion phase in the Franz diffusion cell system, from which flux (J) and permeability coefficients (Kp) were calculated. Further samples collected at later time intervals (12–48 h) were used to evaluate compound stability and long-term permeation behavior.

The parent compounds showed observable transmembrane diffusion with flux values ranging from 3.82 to 7.34 $\mu g \cdot h^{-1} \cdot cm^{-2}$ and corresponding permeability coefficients (Kp) of 1.38 to 3.00 × 10^{-3} $cm \cdot h^{-1}$ Table 2.

In contrast, the penetration of the galactosylated derivatives was significantly lower. Receptor chamber samples showed weak chromatographic signals, but under the experimental conditions, their concentrations remained below the measurable range, making it difficult to accurately measure flux and Kp values.

It should be noted that possible compound retention inside the Strat-M™ membrane was not assessed because the present study focused on compound penetration into the receptor phase. Future studies involving membrane extraction and HPLC analysis would provide insight into potential chemical retention in the artificial skin layer.

All things considered, these findings show that galactosylation significantly reduces transdermal transport compared to the parent preservatives, showing a decreased risk of systemic exposure as shown in Figure 6.

 doi:10.20944/preprints202605.0095.v1

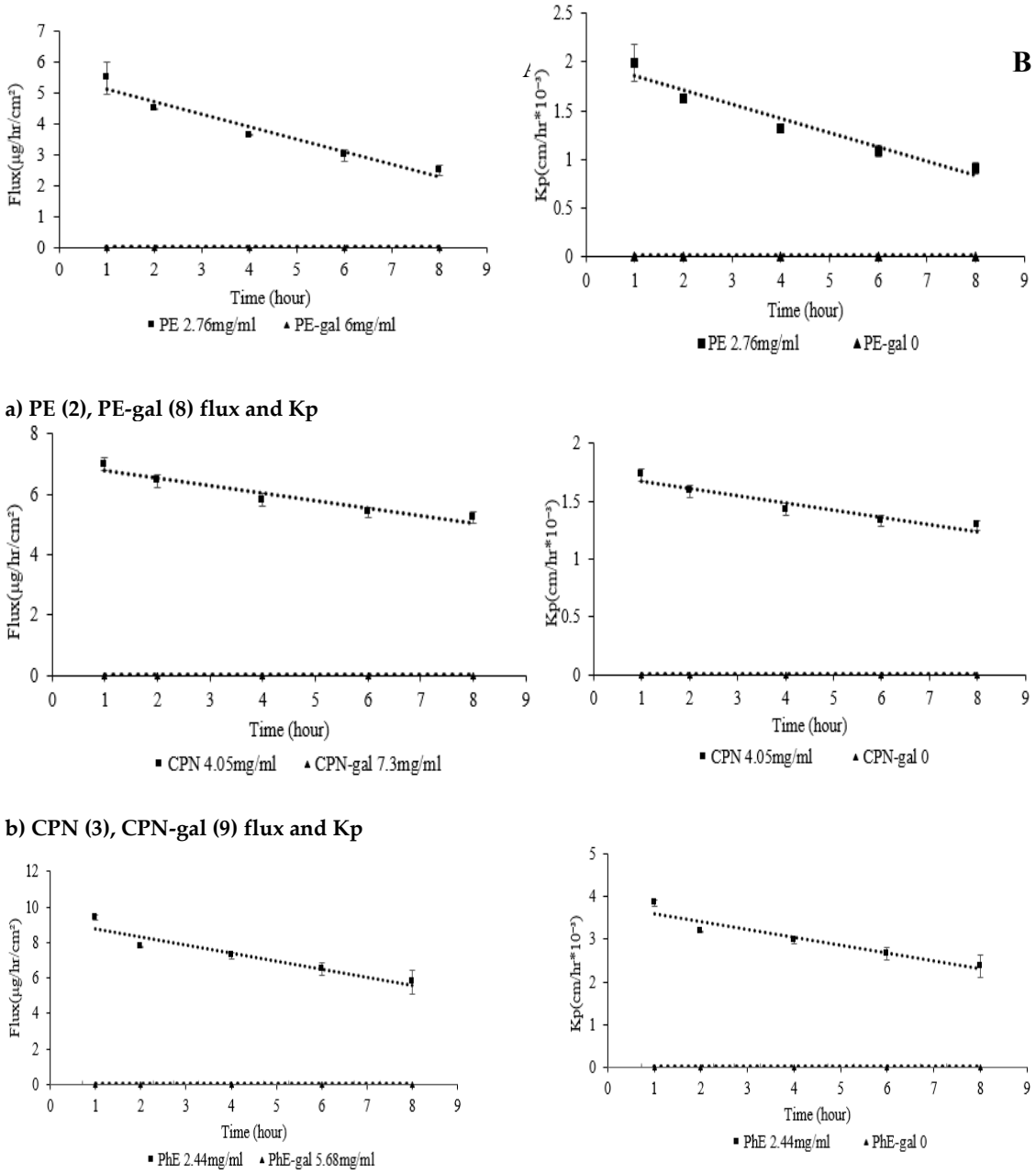

Figure 6. Transdermal flux (A) and permeability coefficients (Kp) (B) of the parent compounds and their galactosylated derivatives across Strat-M™ membranes at 32°C. Flux values were calculated from the initial linear region of the permeation profile (0–8 h) obtained in Franz diffusion cell experiment.

Table 2. Steady-state flux and permeability coefficients (Kp) of non-galactosylated preservatives and galactosylated derivatives across Strat-M™ membranes.

Compound	Flux (μg h⁻¹ cm⁻²)	Kp (cm·h⁻¹ ×10⁻³)
PE	3.82	1.38
CPN	5.97	1.47
PhE	7.34	3.00
PE-gal	0	0
CPN-gal	0	0
PhE-gal	0	0

 doi:10.20944/preprints202605.0095.v1

4.4. Cytotoxicity Assessment of Non-Galactosylated and Galactosylated Derivatives Using LD_{50} Values

The LD_{50} values showed a significant reduction in cytotoxicity upon galactosylation for all the original compounds. Among them, 2-phenoxyethanol (Figure 7 E) showed the highest toxicity with an LD_{50} of 0.1 mg/mL, followed by 2-phenylethanol (Figure 7 D, 0.12 mg/mL), chlorphenesin (Figure 7 C, 0.13 mg/mL), 1,2-octanediol (Figure 7 B, 0.16 mg/mL), and 1,2-hexanediol (Figure 7 A, 0.79 mg/mL). After galactosylation, the LD_{50} values increased significantly: 2-phenoxyethanol-gal (2.1 mg/mL), 2-phenylethyl-gal (1.9 mg/mL), chlorphenesin-gal (1.6 mg/mL), 1,2-octanediol-gal (1.90 mg/mL), and 1,2-hexanediol-gal (1.77 mg/mL). This increase shows that galactosylation effectively decreases the bioactivity of these cosmetic preservatives.

Galactosylated derivatives consistently show higher LD_{50} values compared to their corresponding non galactosylated compounds, a meaningful reduction in cytotoxicity upon galactosylation. The cytotoxicity of non galactosylated compounds (A–E) and their galactosylated derivatives (A1–E1) was quantitatively evaluated to determine the protective effect of galactosylation in Figure 7.

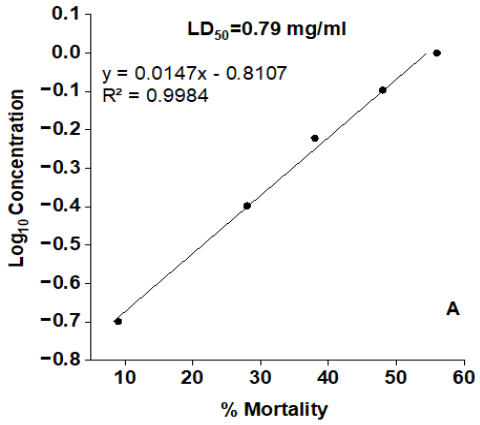

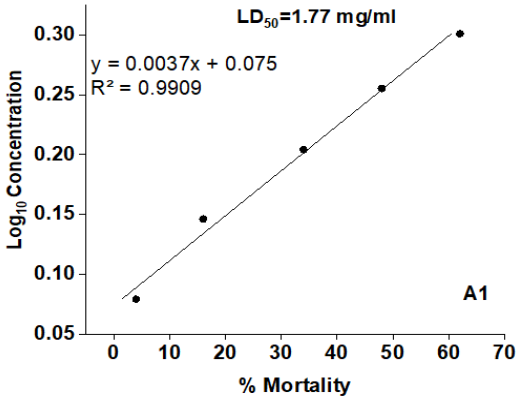

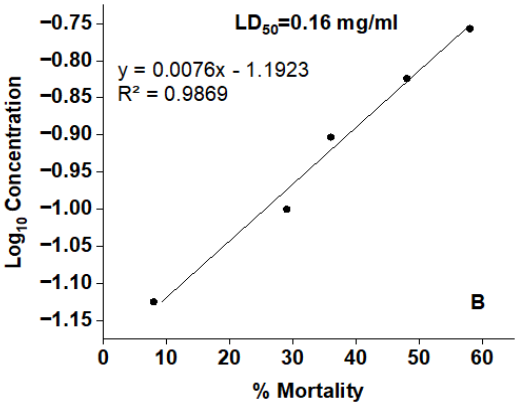

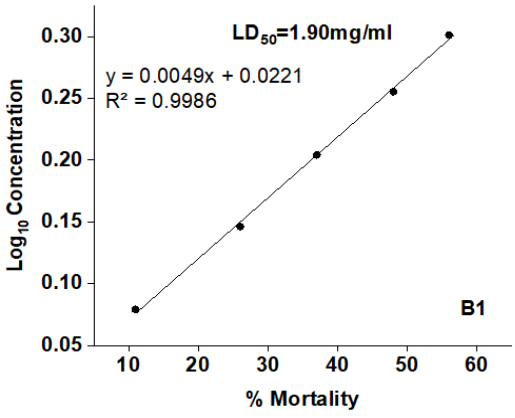

 doi:10.20944/preprints202605.0095.v1

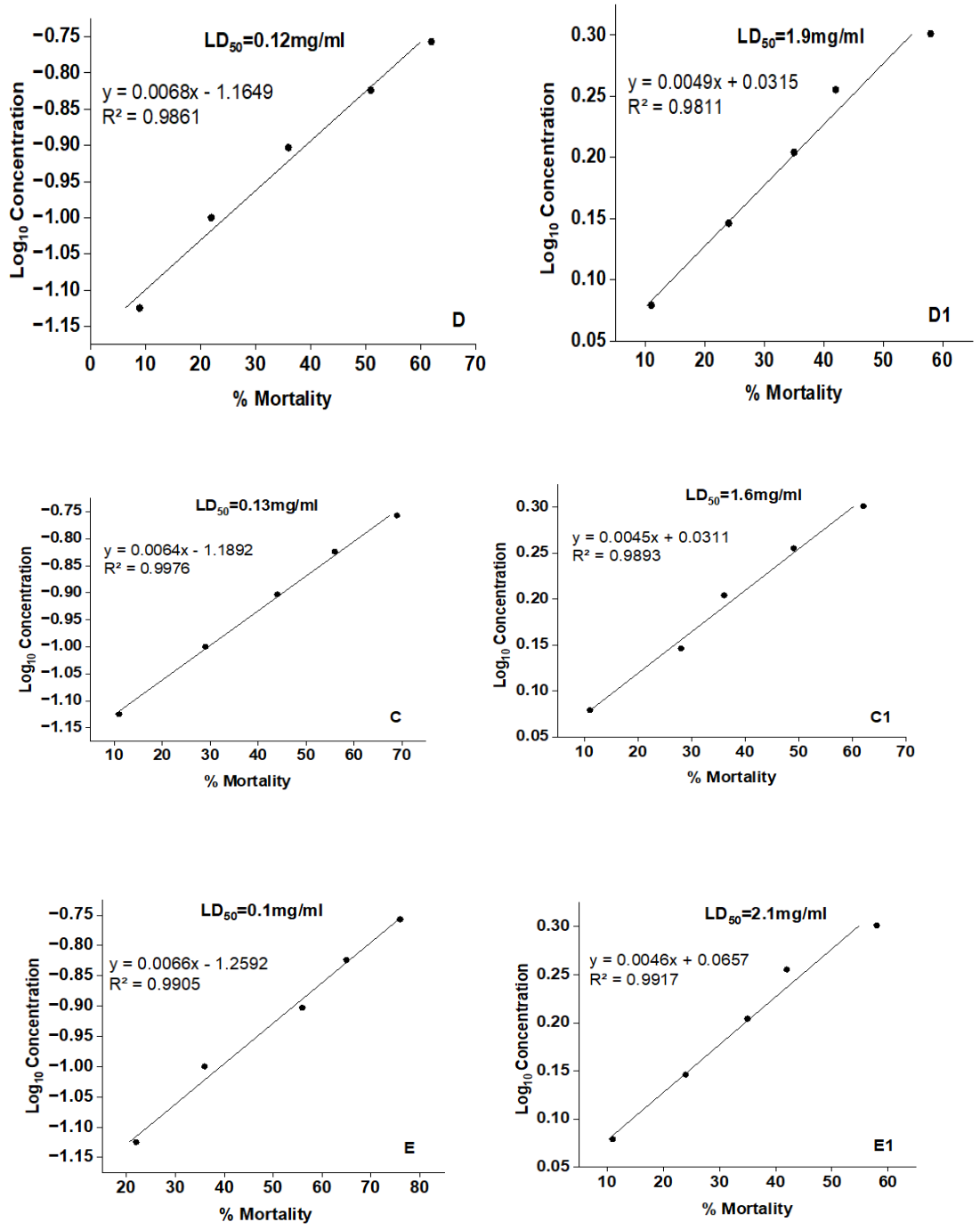

Figure 7. Brine shrimp lethality assay showing cytotoxic effects of original and galactosylated compounds. LD_{50} values of the original compounds (A–E) and their galactosylated derivatives (A1–E1) after 24 hours of incubation (three replicates per experiment). **A:** 1,2-hexanediol; **A1:** 1,2-hexanediol-gal; **B:** 1,2-octanediol; **B1:** 1,2-octanediol-gal; **C:** chlorphenesin; **C1:** chlorphenesin-gal; **D:** 2-phenylethanol; **D1:** 2-phenylethanol-gal; **E:** 2-phenoxyethanol; **E1:** 2-phenoxyethanol-gal.

Experimental variation supports the hypothesis that conjugation of the galactose moiety reduces membrane permeability and bioavailability, thereby lowering the toxicologic risk related to dermal contact. These results specify that galactosylated compounds play a fundamental role in reducing toxicity, making them potentially safe for biological applications in the cosmetic industry.

 doi:10.20944/preprints202605.0095.v1

5. NMR Characterization of β-D-Galactopyranoside Derivatives

Samples were applied to a high-speed liquid chromatography-mass spectrometer (LCMS-IT-TOF, Shimadzu Corp., Tokyo, Japan). ^{1}H and ^{13}C-NMR were performed on a Bruker DRX400 NMR spectrometer (400 MHz). The structures of the synthesized galactosylated derivatives were confirmed by ^{1}H and ^{13}C NMR spectroscopy. The ^{1}H NMR spectrum of BnO-gal **7** displays multiple resonances consistent with galactosylation of benzyl alcohol. Downfield signals at δ_H 7.43–7.24 ppm indicate the presence of the aromatic ring of the benzyl moiety. The benzylic CH_2 appears as two distinct signals at δH 4.93 and 4.67 ppm, which is attributed to diastereotopic splitting arising from interaction with the bulky, substituted sugar, despite the CH_2 not being adjacent to a chiral center. Characteristic carbohydrate resonances are observed at δH 4.32, 3.84, and 3.82–3.46 ppm, corresponding to seven protons, thereby supporting the attachment of a galactose unit to benzyl alcohol. The ^{13}C NMR spectrum shows a total of eleven carbon signals derived from the BnO-gal structure, comprising four aromatic carbons, one benzylic CH_2 carbon, and six carbohydrate carbons within δC 76.9–62.7 ppm. This data confirm that the compound is a benzyl glucoside bearing a single sugar substituent. Compounds **8**~**12** likewise exhibit ^{1}H NMR and ^{13}C NMR signals characteristic of galactosylation of the parent alcohols, clearly demonstrating that the original preservatives have been conjugated with a sugar moiety. The corresponding spectra of BnO-gal, CPN-gal, HDO-gal, OD-gal, and PhE-gal are provided in supplementary Information (Figures S3–S12).

5.1. Benzyl β-D-Galactopyranoside (7)

[108.14 (BnOH) + 180.156 (galactose) - 18.015 (water) + 22.99 (Na^+) = 293.271] [$C_{13}H_{18}NaO_6$]. ^{1}H NMR (400 MHz, CD_3OD) 7.43~7.41 (d, 2H, *J*=7.2 Hz), 7.34~7.30 (t, 2H, *J*=7.2 Hz), 7.28~7.24 (m, 1H), 4.93 (d, 1H, *J*=12.0 Hz), 4.67 (d, 1H, *J*=12.0 Hz), 4.32 (d, 1H, *J*=7.6 Hz), 3.84 (d, 1H, , *J*=3.2 Hz), 3.82~3.72 (m, 2H), 3.59 (t, 1H, *J*=9.2 Hz), 3.51 (t, 1H, *J*=6.0 Hz), 3.46 (dd, 1H, *J*=10.0 Hz, , *J*=3.6 Hz). ^{13}C NMR (100 MHz, CD_3OD) 139.3, 129.4, 129.3, 128.8, 104.0, 76.9, 75.1, 72.7, 71.8, 70.5, 62.7.

5.2. 2-Phenoxyethanol β-D-Galactopyranoside (8)

LC-MS (ESI): m/z $C_{14}H_{20}O_7$, theoretical exact mass, 300.1; measured mass, 323.1 ([M+Na]$^+$) and 299.1 ([M-H]$^-$). ^{1}H NMR (400 MHz, D_2O) δ 7.34 (m, 2H), 7.01 (m, 3H), 4.42 (d, 1H, J = 8 Hz), 4.22 (t, 2H, J = 4 Hz), 4.19 (m, 1H), 3.98 (m, 1H), 3.86 (d, 1H, J = 4 Hz), 3.69 (m, 2H), 3.64 (t, 1H, J = 4 Hz), 3.60 (dd, 1H, J = 12 Hz, J = 4 Hz), 3.50 (dd, 1H, J = 12 Hz, J = 8 Hz). ^{13}C NMR (100 MHz, D_2O) δ 157.8, 129.9, 121.7, 114.9, 103.0, 75.1, 72.7, 70.8, 69.2, 68.2, 67.4, 60.

5.3. Chlorphenesin β-D-Galactopyranoside (9)

Mass (ESI): m/z $C_{15}H_{21}ClO_8Cl$ (M+Cl$^-$); theoretical exact mass, 399.0619; measured mass, 399.0623. ^{1}H NMR (400 MHz, CD_3OD) 7.24 (d, 2H, J=6.6 Hz), 6.94 (d, 2H, J=6.6 Hz), 4.26 (dd, 1H, J=5.7 Hz and 1.8 Hz), 4.12 (m, 1H), 4.08 (m, 1H), 4.03 (m, 1H), 3.99 (m, 1H), 3.83 (d, 1H, *J*=2.4 Hz), 3.78–3.70 (m, 3H), and 3.58–3.47 (m, 3H). ^{13}C NMR (100 MHz, CD_3OD) 157.3, 129.8, 126.1, 116.7, 103.6, 75.6, 73.1,71.3, 71.0, 69.6, 69.1, 69.0, and 61.4.

5.4. 1,2-Hexandiol β-D-Galactopyranoside (10)

[118.174 (1,2-hexanediol) + 180.156 (galactose) - 18.01528 (water) + 1.007276 (H^+) = 281.3219762]. ^{1}H NMR (400MHz, D_2O) 4.44 (d, 1H, *J*=7.7 Hz), 3.96 (d, 1H, *J*=3.0 Hz), 3.92~3.90 (m, 1H), 3.86~3.76 (m, 2H), 3.79 (d, 1H, *J*=4.4 Hz), 3.74~3.70 (m, 2H), 3.68 (d, 1H, *J*=2.9 Hz), 3.58 (t, 1H, *J*=8.8 Hz), 1.60~1.45 (m, 2H), 1.40~1.35 (m, 4H), 0.92 (t, 3H, *J*=6.7 Hz). ^{13}C NMR (100 MHz, D_2O) α-anomer; 103.4, 75.1, 74.2, 72.7, 70.9, 70.5, 68.6, 60.9, 31.9, 26.9, 21.9, 13.2. β-anomer; 102.9, 75.1, 73.9, 72.6, 70.8, 70.2, 68.6, 60.9, 31.9, 26.9, 21.9, 13.2.

 doi:10.20944/preprints202605.0095.v1

5.5. 1,2-Octanediol β-D-Galactopyranoside (11)

Mass (ESI): m/z 281.1601 (m/z) theoretical exact mass [118.174 (1, 2-hexanediol) + 180.156 (galactose) - 18.01528 (water) + 1.007276 (H^+) = 281.3219]. ^{1}H NMR (400MHz, D_2O) 4.39 (d, 2H, *J*=7.6 Hz), 3.98~3.95 (m, 4H), 3.90~3.82 (m, 2H), 3.81~3.77 (m, 6H), 3.71~3.66 (m, 6H), 3.60~3.55 (m, 2H), 1.52~1.42 (m, 4H), 1.36~1.26 (m, 16H), 0.89 (t, 6H, *J*=6.0 Hz). ^{13}C NMR (100 MHz, D_2O) 103.6, 103.0, 75.0, 74.9, 74.4, 74.0, 72.71, 72.66, 70.9, 70.8, 70.5, 70.1, 68.5, 68.4,60.8, 60.6, 32.64, 32.58, 31.4, 29.0, 25.1, 25.0, 22.3, 13.6.

5.6. 2-Phenylethanol β-D-Galactopyranoside (12)

LC-MS (ESI): 307.118 m/z $C_{14}H_{20}NaO_6^+$, theoretical exact mass [122.073 (2-phenylethanol) + 180.063 (galactose) – 18.01 (water) + 22.99 (Na^+) = 307.115]. ^{1}H NMR (400 MHz, D_2O) δ 7.30~7.26 (m, 4H), 7.25~7.21 (m, 1H), 4.31 (d, 1H, *J* = 8.0 Hz), 4.07 (q, 1H, *J* = 8.0 Hz), 3.86~3.81 (m, 2H), 3.71~3.62 (m, 2H), 3.58~3.51 (m, 2H), 3.38 (t, 1H, *J* = 15.8 Hz), 2.88 (t, 2H, *J* = 7.0 Hz). ^{13}C NMR (100 MHz, D_2O) δ 138.7. 129.0, 128.6, 126.5, 102.7, 75.0, 72.7, 70.6, 68.6, 60.9, 35.2.

The present study shows that the biological and physical properties of widely used cosmetic preservatives are considerably changed by enzymatic galactosylation. Specifically, compared to their parent compounds, the conjugation of galactose to 2-phenoxyethanol, chlorphenesin, and 2-phenylethanol led to a significant decrease in transdermal penetration across Strat-M™ membrane. These results are consistent with previous studies showing that galactosylation can significantly affect polarity, molecular size, and membrane permeability.

The ability of parent preservatives, such as phenoxyethanol, chlorphenesin, and phenylethanol, to diffuse across the artificial skin membrane was shown in this research by measured flux values. On the other hand, in receptor chamber samples, their galactosylated derivatives are shown below the limit of quantification (LOQ). This indicates that skin penetration is effectively reduced by the addition of the galactose moiety. The sugar group's steric and polarity effects, which likely restrict diffusion through the membrane's lipid matrix, are responsible for the reduced penetration noticed in this research.

Cytotoxicity and irritation during skin contact are important concerns for the safety of cosmetic preservatives[33]. Reducing the transdermal penetration of preservatives is especially beneficial for cosmetic applications from a formulation perspective. Instead of penetrating deeply into the skin, preservatives are meant to shield the formulation from microbial contamination[34,35].

Galactosylation is a form of glycosylation that can influence molecular polarity, size, and membrane permeability is a chemical change that shows promise for achieving this objective[36,37]. Additionally, previous studies indicate that the antibacterial activity of 2-phenoxyethanol against common bacterial strains such *Enterococcus faecalis*, *Pseudomonas aeruginosa*, *Escherichia coli*, and *Staphylococcus aureus* are not significantly affected by galactosylation[38]. Cytotoxicity experiments using the HaCaT model, which showed that the galactosylated derivative of chlorphenesin exhibits less toxicity than the parent molecule, provide more proof of the safety advantages of galactosylated preservatives[39].

The overall findings show that enzymatic galactosylation offers a useful method for modifying the physicochemical and biological characteristics of cosmetic preservatives. These results demonstrate the possibility of using galactosylated derivatives in cosmetic formulations as safer substitutes for conventional preservatives. To accurately evaluate these compounds' potential for use in cosmetic and dermatological applications, future research must look for their antibacterial activity, long-term stability, and possible membrane retention.

Considering the well-known broad antibacterial properties of the parent preservatives, the antibacterial activity of the galactosylated derivatives was evaluated in our previous research. Furthermore, using mammalian cell lines like HaCaT or 3T3 evaluation of cytotoxicity for more evidence. The Franz diffusion experiment was not performed for BnOH, HD, and OD since they did not yield consistent or quantifiable chromatographic responses under the current HPLC conditions, making reliable permeation analysis unfeasible.

 doi:10.20944/preprints202605.0095.v1

6. Conclusions

The physicochemical and biological properties of 2-phenoxyethanol (PE), 2-phenylethanol (PhE), and chlorphenesin (CPN) were successfully modified by galactosylation. The structures of the synthesized galactosylated derivatives were confirmed using ^{1}H and ^{13}C NMR spectroscopy and High-Performance Liquid Chromatography (HPLC). Furthermore, HPLC analysis showed that the galactosylated derivatives remained chemically stable for 48 hours and exhibited earlier elution rates than their parent compounds, indicating stronger polarity.

Franz Diffusion cell assay showed that galactosylation significantly reduced skin penetration as compared to standard compounds. The non-galactosylated compounds showed quantifiable steady-state flux values (3.82–7.34 $\mu g \cdot h^{-1} \cdot cm^{-2}$) and permeability coefficients (Kp= 1.38–3.00 $\times 10^{-3}$ $cm \cdot h^{-1}$), whereas the galactosylated derivatives showed unquantifiable permeation levels under the experimental conditions.

Furthermore, in *Artemia salina* toxicity tests, the LD_{50} values of the galactosylated derivatives were higher than those of the corresponding standard compounds, indicating a decrease in cytotoxicity. All these results suggest that galactosylation can reduce transdermal penetration while maintaining chemical stability, providing a workable method for the development of safer cosmetic preservatives.

Supporting data: The following supporting information can be downloaded at the website of this paper posted on Preprints.org. The supplementary Information files provide the datasets supporting the results presented in this study Heading 1. These include calibration curves for PE and PE-gal, CPN and CPN-gal, and PhE and PhE-gal, Figure S1. The cytotoxicity data of standard paraben showed in the supplemental data Heading 2 (Figure S2). The Heading 3 (a-e) (Figures S3–S12) contains the ^{1}H and ^{13}C NMR spectra of the synthesized galactosylated derivatives BnO-gal, CPN-gal, HD-gal, OD-gal, and PhE-gal.

Funding: This research was supported by the Regional Innovation System & Education (RISE) program through the (Chungbuk Regional Innovation System & Education Center), funded by the Ministry of Education (MOE) and the (Chungcheongbuk-do), Republic of Korea. (2025- RISE-11-004). This work was supported by the Glocal University 30 Project of the Korea National University of Transportation in 2025.

Acknowledgments: The authors gratefully acknowledge the Department of Biotechnology for providing academic resources and a supportive environment during the preparation of this review article

Conflicts of Interest: The authors declare no conflict of interest, financial or otherwise.

References

1. Z. Tang, Q. Du, Mechanism of action of preservatives in cosmetics, Journal of Dermatologic Science and Cosmetic Technology 1 (2024) 100054. https://doi.org/10.1016/j.jdsct.2024.100054.
2. A.D.P.M. Canavez, G. de Oliveira Prado Corrêa, V.L.B. Isaac, D.C. Schuck, M. Lorencini, Integrated approaches to testing and assessment as a tool for the hazard assessment and risk characterization of cosmetic preservatives, Journal of Applied Toxicology 41 (2021) 1687–1699. https://doi.org/10.1002/jat.4156.
3. P. Poddębniak, U. Kalinowska-Lis, A Survey of Preservatives Used in Cosmetic Products, Applied Sciences 14 (2024) 1581. https://doi.org/10.3390/app14041581.
4. P. Głaz, A. Rosińska, S. Woźniak, A. Boguszewska-Czubara, A. Biernasiuk, D. Matosiuk, Effect of Commonly Used Cosmetic Preservatives on Healthy Human Skin Cells, Cells 12 (2023) 1076. https://doi.org/10.3390/cells12071076.
5. A. Panico, F. Serio, F. Bagordo, T. Grassi, A. Idolo, M. De Giorgi, M. Guido, M. Congedo, A. De Donno, Skin safety and health prevention: An overview of chemicals in cosmetic products, J. Prev. Med. Hyg. 60 (2019) E50–E57. https://doi.org/10.15167/2421-4248/jpmh2019.60.1.1080.
6. P.D. Darbre, A. Aljarrah, W.R. Miller, N.G. Coldham, M.J. Sauer, G.S. Pope, Concentrations of parabens in human breast tumours, Journal of Applied Toxicology 24 (2004) 5–13. https://doi.org/10.1002/jat.958.

 doi:10.20944/preprints202605.0095.v1

7. C.N. Smith, B.R. Alexander, The relative cytotoxicity of personal care preservative systems in Balb/C 3T3 clone A31 embryonic mouse cells and the effect of selected preservative systems upon the toxicity of a standard rinse-off formulation, in: Toxicology in Vitro, 2005: pp. 963–969. https://doi.org/10.1016/j.tiv.2005.06.014.
8. E.R. Valle-González, J.A. Jackman, B.K. Yoon, N. Mokrzecka, N.-J. Cho, pH-Dependent Antibacterial Activity of Glycolic Acid: Implications for Anti-Acne Formulations, Sci. Rep. 10 (2020) 7491. https://doi.org/10.1038/s41598-020-64545-9.
9. A. Kumar, S. Kaur, P.L. Sangwan, S.A. Tasduq, Therapeutic and cosmeceutical role of glycosylated natural products in dermatology, Phytotherapy Research 37 (2023) 1574–1589. https://doi.org/10.1002/ptr.7752.
10. S.S. Shivatare, V.S. Shivatare, C.-H. Wong, Glycoconjugates: Synthesis, Functional Studies, and Therapeutic Developments, Chem. Rev. 122 (2022) 15603–15671. https://doi.org/10.1021/acs.chemrev.1c01032.
11. D. Chettri, M. Chirania, D. Boro, A.K. Verma, Glycoconjugates: Advances in modern medicines and human health, Life Sci. 348 (2024) 122689. https://doi.org/10.1016/j.lfs.2024.122689.
12. A. Koššuthová, M. Antošová, V. Bauerová-Hlinková, J.A. Bauer, M. Polakovič, β-Galactosidase-Catalyzed Transglycosylation of Tyrosol: Substrates and Deep Eutectic Solvents Affecting Activity and Stability, Biomolecules 15 (2025) 801. https://doi.org/10.3390/biom15060801.
13. J. Li, H. Xiang, Q. Zhang, X. Miao, Polysaccharide-Based Transdermal Drug Delivery, Pharmaceuticals 15 (2022) 602. https://doi.org/10.3390/ph15050602.
14. A. Andreu, M. Ćorović, C. Garcia-Sanz, A.S. Santos, A. Milivojević, C. Ortega-Nieto, C. Mateo, D. Bezbradica, J.M. Palomo, Enzymatic Glycosylation Strategies in the Production of Bioactive Compounds, Catalysts 13 (2023) 1359. https://doi.org/10.3390/catal13101359.
15. B.M. de Roode, M.C.R. Franssen, A. van der Padt, R.M. Boom, Perspectives for the Industrial Enzymatic Production of Glycosides, Biotechnol. Prog. 19 (2003) 1391–1402. https://doi.org/10.1021/bp030038q.
16. H.-Y. Lee, K.-H. Jung, 베타-갈락토시데이즈를 이용하여 합성된 Benzyl Alcohol Galactoside 의 NMR Spectroscopy 및 Mass spectrometry NMR Spectroscopy and Mass Spectrometry of Benzyl Alcohol Galactoside synthesized using β-Galactosidase, Journal of the Korean Applied Science and Technology 36 (2019) 84–89. https://doi.org/10.12925/jkocs.2019.36.1.84.
17. H.Y. Lee, K.H. Jung, Enzymatic synthesis of 2-phenoxyethanol galactoside by whole cells of β-galactosidase-containing Escherichia coli, J. Microbiol. Biotechnol. 24 (2014) 1254–1259. https://doi.org/10.4014/jmb.1404.04004.
18. S.E. Lee, H.Y. Lee, K.H. Jung, Production of chlorphenesin galactoside by whole cells of β-galactosidase-containing Escherichia coli, J. Microbiol. Biotechnol. 23 (2013) 826–832. https://doi.org/10.4014/jmb.1211.11009.
19. Y.-O. Kim, H.-Y. Lee, K.-H. Jung, NMR Spectroscopy and Mass Spectrometry of 1, 2-Hexanediol Galactoside synthesized using Escherichia coli β-Galactosidase, Journal of the Korean Oil Chemists' Society 33 (2016) 286–292. https://doi.org/10.12925/jkocs.2016.33.2.286.
20. S. Zsikó, E. Csányi, A. Kovács, M. Budai-Szűcs, A. Gácsi, S. Berkó, Methods to Evaluate Skin Penetration In Vitro, Sci. Pharm. 87 (2019) 19. https://doi.org/10.3390/scipharm87030019.
21. S.E. Lee, T.M. Jo, H.Y. Lee, J. Lee, K.H. Jung, β-Galactosidase-catalyzed synthesis of galactosyl chlorphenesin and its characterization, Appl. Biochem. Biotechnol. 171 (2013) 1299–1312. https://doi.org/10.1007/s12010-013-0213-3.
22. H.J. Byeon, K.H. Jung, G.S. Moon, S.K. Moon, H.Y. Lee, A facile and efficient method for the synthesis of crystalline tetrahydro-β-carbolines via the Pictet-Spengler reaction in water, Sci. Rep. 10 (2020). https://doi.org/10.1038/s41598-020-57911-0.
23. T. Du, Y. Wang, H. Xie, D. Liang, S. Gao, Fragmentation Patterns of Phenolic C-Glycosides in Mass Spectrometry Analysis, Molecules 29 (2024) 2953. https://doi.org/10.3390/molecules29132953.
24. P. He, Y. Shao, S. Zhou, R. Wang, W. Ma, Structural Biology and Analytical Chemistry Approaches for Characterizing C-Glycoside Metabolic Enzymes in Human Gut Microbiota, Journal of Visualized Experiments (2025). https://doi.org/10.3791/67629.

 doi:10.20944/preprints202605.0095.v1

25. L. Chedik, S. Baybekov, F. Cosnier, G. Marcou, A. Varnek, C. Champmartin, An update of skin permeability data based on a systematic review of recent research, Sci. Data 11 (2024) 224. https://doi.org/10.1038/s41597-024-03026-4.
26. Y.G. Anissimov, M.S. Roberts, Diffusion modeling of percutaneous absorption kinetics. 1. Effects of flow rate, receptor sampling rate, and viable epidermal resistance for a constant donor concentration, J. Pharm. Sci. 88 (1999) 1201–1209. https://doi.org/10.1021/js990053i.
27. B. Liang, L. Zhou, C. Wu, L. Fang, L. Wang, L. Peng, P. Shu, L. Tang, Y. Bei, X. Cui, X. Chen, Y. Gao, C. Han, Y. Jia, H. Lin, Y. Li, Y. Liu, Y. Li, Z. Li, Z. Liu, S. Ren, J. Shi, W. Sun, L. Tian, Q. Wang, Y. Wang, Y. Xu, M. Zeng, Q. Zhu, S. Zhang, Y. Zhang, Q. Xiang, Expert consensus on the technical specifications of the in vitro skin penetration test of cosmetic product by Franz diffusion cell, Journal of Dermatologic Science and Cosmetic Technology 1 (2024) 100040. https://doi.org/10.1016/j.jdsct.2024.100040.
28. C.N. Banti, S.K. Hadjikakou, Evaluation of toxicity with brine shrimp assay, Bio. Protoc. 11 (2021). https://doi.org/10.21769/BioProtoc.3895.
29. J.M. Da Silveira Carvalho, A.H. De Morais Batista, N.A.P. Nogueira, A.K.M. Holanda, J.R. De Sousa, D. Zampieri, M.J.B. Bezerra, F. Stefânio Barreto, M.O. De Moraes, A.A. Batista, A.C.S. Gondim, T.D.F. Paulo, L.G. De França Lopes, E.H.S. Sousa, A biphosphinic ruthenium complex with potent anti-bacterial and anti-cancer activity, New Journal of Chemistry 41 (2017) 13085–13095. https://doi.org/10.1039/c7nj02943h.
30. A.F.A. Trompeta, I. Preiss, F. Ben-Ami, Y. Benayahu, C.A. Charitidis, Toxicity testing of MWCNTs to aquatic organisms, RSC Adv. 9 (2019) 36707–36716. https://doi.org/10.1039/c9ra06672a.
31. B. Zhu, S. Zhu, J. Li, X. Hui, G.-X. Wang, The developmental toxicity, bioaccumulation and distribution of oxidized single walled carbon nanotubes in *Artemia salina*, Toxicol. Res. (Camb). 7 (2018) 897–906. https://doi.org/10.1039/C8TX00084K.
32. S. Waghulde, M.K. Kale, VijayR. Patil, Brine Shrimp Lethality Assay of the Aqueous and Ethanolic Extracts of the Selected Species of Medicinal Plants, in: MDPI AG, 2020: p. 47. https://doi.org/10.3390/ecsoc-23-06703.
33. L. Shen, J. Lin, J. Lin, W. Wu, Glycosylation in Dermatology: Unveiling the Sugar Coating of Skin Disease, Exp. Dermatol. 34 (2025). https://doi.org/10.1111/exd.70098.
34. C. Das, P.D. Olmsted, M.G. Noro, Water permeation through stratum corneum lipid bilayers from atomistic simulations, Soft Matter 5 (2009) 4549. https://doi.org/10.1039/b911257j.
35. M. Yokota, Y. Tokudome, Permeation of Hydrophilic Molecules across Glycated Skin Is Differentially Regulated by the Stratum Corneum and Epidermis–Dermis, Biol. Pharm. Bull. 38 (2015) 1383–1388. https://doi.org/10.1248/bpb.b15-00372.
36. J. Danzberger, M. Donovan, C. Rankl, R. Zhu, S. Vicic, C. Baltenneck, R. Enea, P. Hinterdorfer, G.S. Luengo, Glycan distribution and density in native skin's stratum corneum, Skin Research and Technology 24 (2018) 450–458. https://doi.org/10.1111/srt.12453.
37. W.M. Holleran, Y. Takagi, G.K. Menon, G. Legler, K.R. Feingold, P.M. Elias, Processing of epidermal glucosylceramides is required for optimal mammalian cutaneous permeability barrier function., Journal of Clinical Investigation 91 (1993) 1656–1664. https://doi.org/10.1172/JCI116374.
38. K.-H. Jung, H.-Y. Lee, Escherichia coli β-galactosidase-catalyzed synthesis of 2-phenoxyethanol galactoside and its characterization, Bioprocess Biosyst. Eng. 38 (2015) 365–372. https://doi.org/10.1007/s00449-014-1276-4.
39. S.-E. Lee, T.-M. Jo, H.-Y. Lee, J. Lee, K.-H. Jung, β-Galactosidase-Catalyzed Synthesis of Galactosyl Chlorphenesin and Its Characterization, Appl. Biochem. Biotechnol. 171 (2013) 1299–1312. https://doi.org/10.1007/s12010-013-0213-3.